Eur. J. Biochem. **268**, 4278–4284 (2001) © FEBS 2001

Crumpled structure of the custom hydrophobic lytic peptide cecropin B3

S. Srisailam[1], T. K. S. Kumar[1], A. I. Arunkumar[2], K. W. Leung[3], C. Yu[1] and H. M. Chen[4]

[1]*Department of Chemistry, National Tsing Hua University, Hsinchu, Taiwan;* [2]*Department of Biochemistry, Vanderbilt University, Nashville, TN, USA;* [3]*Department of Biochemistry, Hong Kong University of Science and Technology, Hong Kong;* [4]*Institute of BioAgricultural Sciences, Academia Sinica, Taipei, Taiwan*

The solution structure of a custom lytic peptide, cecropin B3 (CB3), having two identical hydrophobic segments on both the N- and C-termini, was investigated by two-dimensional NMR spectroscopy. The need to determine the structure of this peptide is rooted in its specific ability to lyse lipid layers that have a high content of anionic lipid. The lytic activities of CB3 on cell membranes including cancer cells and bacteria is found to be less than cecropin B1. The results show that CB3 has four discrete segments forming α helical structures. The crumpled structure of CB3 provides evidence for the lysis of the lipid layer being via a pathway that differs from pore formation. The results in this study provide strong clues towards a rational design for a potent antimicrobial and antitumor peptide.

Keywords: crumpled; NMR structure; cecropin B3.

Every organism has an active system of defense and offense to contend with invaders and predators. In particular, the enormous evolutionary success of insects can be attributed to their ability to produce a rapid and effective response against invading pathogens [1–3]. This response includes the secretion from the hemolymph of polypeptides that have a wide spectrum of antibiotic activities [4]. Among the most extensively studies of these defensive polypeptides are the cecropins from *Hyalophora cecropia*, which possess potent antimicrobial and antimalignant activities [5–7].

Cecropins derived from insect sources belong to a family of homologous peptides of 35–39 amino acids in length [6,8]. In general, cecropins are polar molecules with a primary sequence consisting of a highly basic N-terminus followed by a hydrophobic C-terminus [9]. Studies based on synthetic cecropins reveal that deletion of the first two amino acids at the N-terminal end or replacement of the highly conserved tryptophan at position 2 causes a drastic decrease in antibacterial activity [10]. These peptides, like many other membrane-active peptides, exist predominantly as a random coil in free solution and form a helical conformation in the membrane mimetic environments [11,12]. Solution structures of cecropins A and P1 in helical-promoting solvents were determined recently using two-dimensional NMR spectroscopy [13,14]. Cecropin A was found to have two α helices. The N-terminal helix is highly amphipathic and the cationic residues located in the segment are believed to facilitate binding to acidic lipids through electrostatic interactions in the cell membrane [15]. It is postulated that the hydrophobic C-terminal helix aids in the insertion of the peptide into the membrane [16]. Both N- and C-terminal helical segments in cecropin A are strongly implicated in the biological activity of insect cecropins [17]. The mammalian cecropin P1 was found to fold into a continuous helix, as determined by a view of its whole length, but local potential bend-forming sites between the amphipathic and hydrophobic segments can also be found [14].

The correlation between peptide structure and membrane-lysis pathways has been studied [16,18,19]. Some reports support the idea that cecropins approach the lipid bilayers by adopting their helical conformation, subsequently oligomerizing and aggregating to form 'pores' [16,18]. The formation of such pores causes the leakage of internal components of the cell and leads to cell death. An alternative model proposes a detergent-like action for cecropins [18,19]. Due to their hydrophobic structure, these peptides are believed to flip-flop with the lipid bilayers, disrupting their organization and subsequently causing membrane lysis. Although no clear consensus has been reached so far by relating membrane lysis to the mode of action of lytic peptides, there is growing evidence that the helical structure of cecropins largely contributes to their ability to kill various types of cells [17,20].

Just as it is important to clarify the structure–function relationship for antimicrobial peptides, it is also essential to ascertain the structure–mode-of-action relationship for these peptides before membrane lysis can be understood. Considerable effort is now being made to understand the structure–mode-of-action relationship of cecropins. We have recently designed two analogs of cecropin B (CB) that have the highest antibacterial activity in the cecropin family [21]; cecropin B1 (CB1) possesses two amphipathic helices and cecropin B3 (CB3) has two hydrophobic

Correspondence to H. M. Chen, Institute of BioAgricultural Sciences, Academia Sinica, Taipei, Taiwan. Fax: + 886 2 2651 5600, Tel.: + 886 2 2651 5747, E-mail: robell@gate.sinica.edu.tw, or to C. Yu, Fax: + 886 35 711082, Tel.: + 886 35 721524, E-mail: cyu@mx.nthu.edu.tw

Abbreviations: AOT, aerosol sodium *bis*(2-ethylhexyl) sulfosuccinate; CB, cecropin B; CB1, cecropin B1; CB3, cecropin B3; HE_{50}, concentration of peptide (CB3 or CB1) at which hemolysis is 50%; HFP, 1,1,1,3,3,3-hexafluoro-isopropanol; IC_{50}, concentration of peptide (CB3 or CB1) at which cell viability is 50%; LC, lethal concentration.

(Received 8 May 2001, accepted 8 June 2001)

helices. Based on our experimental observations, compared to CB, CB1 not only killed more cancer cells but also induced different morphological changes in *Klebsiella pneumoniae* and HL-60 leukemia cells [22]. The efficacy of the membrane lysis induced by CB and its analogs on liposomes of different composition was also found to be different [23]. It is believed that the orientation of the helices within the three-dimensional structures of these cecropins in lipid bilayers could be an important contributing factor to the different activities of CB1 [24] and CB3. In this study, we attempt to rationalize a particular lysing pathway for CB3 with its crumpled structure. The different activities of CB3 and CB1 with regard to reversed micelles, cancer cells and bacteria were investigated.

MATERIALS AND METHODS

Materials

The cancer cell lines, HL-60, K-562, Jurkat (E6-1) and CCRF-CEM, as well as fibroblast cells, 3T3 and 3T6, were purchased from American Type Culture Collection. Cell culture media such as F-12 nutrient mixture, fetal bovine serum and Dulbecco's modified Eagle's medium were obtained from Gibco, USA. Analytical grades of penicillin, streptomycin, gentamycin and 1,1,1,3,3,3-hexafluoroisopropanol (HFP) were purchased from Sigma. A microtetrazolium assay kit was obtained from Boehringer Mannheim. Aerosol sodium *bis*(2-ethylhexyl) sulfosuccinate (AOT) with a purity larger than 99% was purchased from Fluka. The fluorescent dye, calcein, was a product of Behring Diagnostics. Sodium 3-(trimethyl silyl)[2,2,3,3,-^{2}H] propionate (99.5% purity), deuterated water (D_2O) (99.9% purity) and deuterated hexafluoroisopropanol (d_2-HFP; 98% purity) were purchased from Cambridge Isotope Laboratory, Andover, MA, USA. The water used in this experiment was deionized and distilled.

Peptide synthesis

Peptides CB3 and CB1 were produced by an ABI 431 peptide synthesizer as previously described [8]. The peptide content was calculated by performing quantitative amino-acid analysis with norleucine as an internal reference amino acid. The purity of the peptide was measured by HPLC. The results for CB3 and CB1 showed that their purity/content were 96%/76% and 98%/73%, respectively. Both amino-acid composition and molecular mass were determined by mass spectrometry. The data (number of amino acids/molecular mass) for CB3 and CB1 were 36/3558 and 34/4113, respectively. These results agree well with the peptide primary sequence. After purification, the peptide solution was lyophilized and a microbalance (Sartourius Research, model R200D) was used to measure the weight of the dried products (± 0.01 mg). The net weight of each peptide was calculated by multiplying the raw weight by the purity and peptide content. The concentration of peptide stock solution was determined from the net weight of peptide and its molecular mass. Amino-acid sequences of CB3 and CB1 were as follows: CB3, (NH_2)-AIAVLGEAKALMGRNIRNGIVKAGPAIAVLGEAKAL-$CONH_2$ and CB1, (NH_2)-KWKVFKKIEKMGRNIRNGIVKAGPKWKVFKKIEK-$CONH_2$. Two identical hydrophobic segments were designed for CB3 (underlined) and two identical amphipathic segments were designed for CB1 (underlined). These peptides are both derived from the natural CB [23].

Encapsulated-dye reversed micelles

Reversed micelles are defined as soluble aggregates of amphiphilic molecules that may spontaneously and reversibly form from monomers in nonpolar solvents. In this experiment, an anionic lipid surfactant, AOT, was used to form reversed micelles with isooctane. A fluorescent probe, calcein dye, was encapsulated in the reversed micelles. The final concentration of AOT (4 mg AOT dissolved in 5 mL isooctane and 150 μL of calcein in $NaCl/P_i$) was ≈ 1.7 mM, which is higher than the critical micelle concentration (0.6–0.9 mM for AOT in isooctane). Detailed descriptions of the reversed micelles are given elsewhere [25]. Triton-100, a strong detergent, was used as a standard to set up a 100% dye leakage from AOT/isooctane reversed micelles.

Assays

The IC_{50} values (concentration of peptide at which cell viability is 50%) of CB3/CB1 on leukemia cells, HL-60, K-562, Jurkat (E6-1) and CCRF-CEM as well as fibroblast cells, 3T3 and 3T6, were measured. The HE_{50} values (concentration of peptide at which hemolysis is 50%) of CB3/CB1 were investigated on fresh venous blood erythrocytes in EDTA solution. The lethal concentration (LC) values of CB3/CB1 on bacteria, *K. pneumoniae*, *Escherichia coli*, and *Pseudomonas aeruginosa*, were determined. The detailed procedures of the above assays can be found in our previous report [8].

CD spectroscopy

CD spectra of CB3 were obtained by using a spectropolarimeter (Jasco Model J-720). Water-jacketed quartz cells with a light path of 1 mm were used to investigate the secondary structure of peptide with 20% (v/v) of HFP providing a membrane-like environment. The peptide concentration was 0.07 mg·mL^{-1} and the solution pH was adjusted to 4.1 in a 2.5-mM sodium phosphate buffer. A detailed description of the CD measurements has been given previously [8].

Preparation of NMR sample

The samples for the NMR experiments were prepared by dissolving 4.8 mg of CB3 in a mixture containing 350 μL of H_2O/D_2O (95 : 5) and 20% of d_2-HFP. This yields a final concentration of 2 mM CB3 in 500 μL. The pH was adjusted to 4.1. A trace of 3-(trimethyl silyl)[2,2,3,3,-2H] propionate was used as an internal standard for NMR spectroscopy.

NMR spectroscopy

All NMR experiments were carried out on a 600-MHz Bruker DMX-600 spectrometer. A two-dimensional ^{1}H-TOCSY [26,27] spectrum using a mixing time of 70 ms was recorded with 64 scans. Similarly, two-dimensional ^{1}H-NOESY spectra using different mixing

times at 50 ms, 125 ms, 200 ms and 250 ms were recorded with 88 scans. Both TOCSY and NOESY spectra were recorded in the time-proportional phase incrementation phase-sensitive mode with presaturation during mixing and relaxation delay [28]. All spectra were recorded at 32 °C.

Structure calculation

The structure calculation was initiated from a linear structure of CB3 obtained using the CHEMNOTE interface of QUANTA 97.0, obtained by input of the CB3 sequence. A parameter structure file derived from a linear protein data bank was then used to generate 50 random structures on a SGI Silicon Graphics O2 workstation using X-PLOR [29,30]. These 50 random structures were then subjected to simulated annealing procedures followed by subsequent refinement steps [29,30] based on 350 experimental NOEs with appropriate pseudo-atom corrections made for methylene and methyl protons [31]. The structure calculation was carried out using a simulated annealing protocol: 20-ps molecular dynamics at 1000 K was followed by 10-ps molecular dynamics. The system was cooled to 100 K over 15 ps and the structures were further refined. The structures were then subjected to 200 cycles of energy minimization by restraint Powell energy minimization based on the CHARMM program [32]. A total of 12 well defined structures with a rmsd were selected from 50 refined structures. All minimization and dynamic simulated annealing calculations were carried out based on the protocol of Nilges *et al.* [33,34]. The final averaged structure was displayed using QUANTA 97.0 software.

RESULTS

Lysis of monolayer reversed micelles induced by CB3 and CB1

Lysis of AOT/isooctane reversed micelles with encapsulated calcein was investigated by the addition of CB3 or CB1 at different concentrations. An increase of fluorescence upon the addition of the lytic peptide implies an increase in calcein leakage from the reversed micelles. Figure 1 shows dye leakage vs. the concentrations of CB3 (filled circles) and CB1 (open circles). The lytic ability of CB3 on the anionic lipid monolayer is greater than that of CB1. Dye leakage is complete (100%) at 4 μM with CB3. However, the maximum dye leakage with CB1 is ≈ 84% at 4 μM.

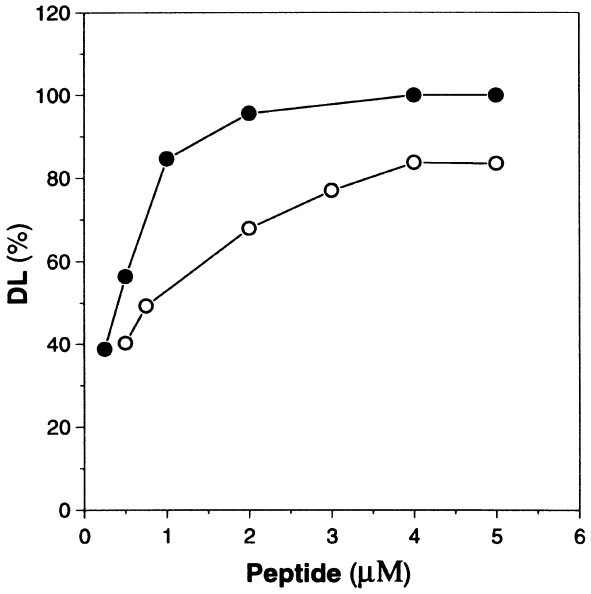

Fig. 1. Monolayer lysis by CB3 (filled circles) and CB1 (open circles) on AOT/isooctane reversed micelles. Calcein dye encapsulated in the reversed micelles was used as a probe to calculate the proportion of dye leakage. DL, dye leakage.

Anticancer and antibacterial activities of CB3 and CB1

The IC_{50} values for CB3 with cancer cells, HL-60, K-562, Jurkat (E6-1), and CCRF-CEM, as well as fibroblast cells, 3T6 and 3T3, were >50 μM. For erythrocytes, the HE_{50} of CB3 was >150 μM. The results indicate that CB3 has little potency on normal and abnormal cells. For CB1, however, the potency on cancer cells is much higher than that on normal cells. Similar results indicating the different potencies of CB3 and CB1 on bacteria such as *K. pneumoniae*, *E. coli*,

Table 1. Measurements of the IC_{50} values of CB3/CB1 on leukemia cells and the lethal concentration (LC) of CB3/CB1 on Gram-negative bacteria. The IC_{50} is the concentration of peptide (CB3 or CB1) at which cell viability is 50%; the HE_{50} is the concentration of peptide (CB3 or CB1) at which hemolysis is 50%. The results are the average of at least three experiments and the average deviations are shown. The IC_{50} and LC data for CB1 were obtained from our previous reports ([24] and [8], respectively). The unit used for the IC_{50} values and the LCs is μM. ND, not determined (e.g. CB3 does not lyse bacteria).

Cell lines	IC_{50} (CB3)	IC_{50} (CB1)	Bacteria	LC (CB3)	LC (CB1)
HL-60	> 50	7.5 ± 0.5	*K. pneumoniae*	ND	0.39 ± 0.015
K-562	> 50	10.2 ± 0.7	*E. coli*	ND	0.49 ± 0.002
Jurkat (E6-1)	> 50	2.4 ± 0.3	*P. aeruginosa*	ND	1.48 ± 0.021
CCRF-CEM	> 50	8.6 ± 0.5			
Fibroblast cells					
3T6	> 50	> 50			
3T3	> 50	> 50			
Erythrocytes	> 150	> 100			

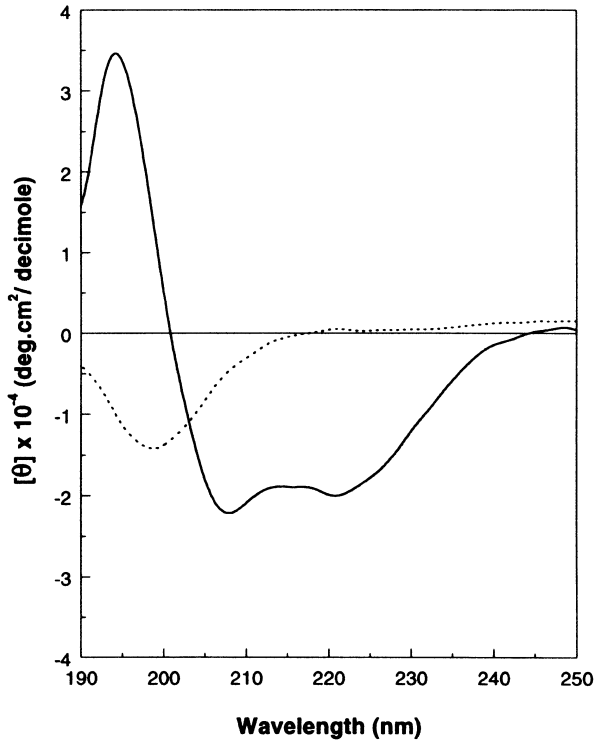

Fig. 2. CD spectra of CB3 with 20% HFP (solid line) and without HFP (dotted line).

and *P. aeruginosa* were obtained. CB3 did not lyse bacteria. A summary of the measurements of the IC_{50} values of CB3/CB1 on leukemia cells and the LCs of these peptides for Gram negative bacteria is shown in Table 1.

CD spectra of CB3

To verify the NMR structure, CD spectra of CB3 were obtained. Figure 2 shows CD spectra of CB3 in the presence (solid line) and absence (dotted line) of 20% (v/v) HFP. CB3 in aqueous solution exists in a random coil conformation. However, upon addition of 20% (v/v) HFP, the peptide assumes a helical conformation as evidenced from the 222 nm and 208 nm negative minimum bands. About 50% of the backbone in CB3 is estimated to exist in a helical conformation in 20% (v/v) HFP.

Sequential assignment

Spin patterns for each amino acid were identified based on a TOCSY spectrum collected with a mixing time of 70 ms. Unambiguous and nearly complete ^{1}H-resonance assignments were achived using the combined information from the TOCSY and NOESY spectra obtained at various mixing times and chemical shifts. Sequential assignment of the residues in the peptide was achieved using the NOESY spectrum obtained with a mixing time of 200 ms. Sequential connectivity (NH-αH) from residue 3 to residue 24 and from residue 26 to residue 36 was unambiguously established. Pro25 was found to occur in a *trans* configuration as shown by the observation of a cross peak obtained from an α proton of Gly24 and a δ proton of Pro25. The identification of helical conformation in CB3 has been accomplished by the connectivity of d_{NN} (i, i + 1) and d_{NN} (i, i + 2). The helical formation in the backbone of CB3 was characterized by the presence of strong d_{NN} (i, i + 1) and medium-range $d_{\alpha\beta}$ (i, i + 3) NOEs among the residues participating in the secondary structure formation. A summary of NOEs substantiating the medium-range interactions in the backbone of CB3 is shown in Fig. 3. Based on the NOE data, it was found that the helical conformation in CB3 is discontinuous and occurs in several sections: residues 4–5, residues 8–9, residues 14–21, residues 26–30 and residues 34–35. The α-proton chemical shift index plot [35] of CB3 also clearly shows that the helix conformation in the protein is not continuous (Fig. 4). In marked contrast, the α-proton chemical shift index plot of the homologous cecropin analog, CB1 [24], reveals that the helical conformation in the peptide exists in only two defined segments (Fig. 4).

Structure calculation

The structure of CB3 was calculated based on 350 distance constraints derived from the information in the NOESY spectra of the peptide obtained at various mixing times (50, 125, 200 and 250 ms). Structure calculation based on distance constraints and further refinement using the simulated annealing technique yielded 12 overlapping structures of CB3. The backbone conformation in the peptide is well defined with an rmsd of 0.93 Å. The Ramachandran plot characterizing the peptide backbone angles (ϕ and ψ) shows that most of the residues fit into the allowed conformational regions. Those that are found in the disallowed regions of the plot mostly correspond to residues in the disordered regions of the structure of CB3. The average structure of CB3 depicts that the helical conformation is discontinuous (Fig. 5). A prominent kink could be

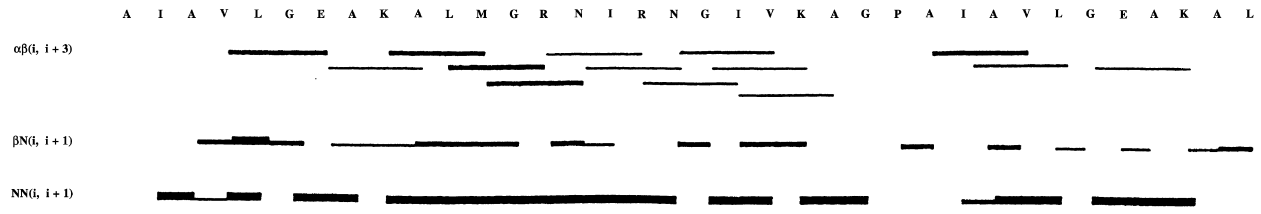

Fig. 3. Schematic representation of the medium-range interactions of NOEs observed for CB3 in 20% HFP. NOE intensities are indicated by the thickness of the bars.

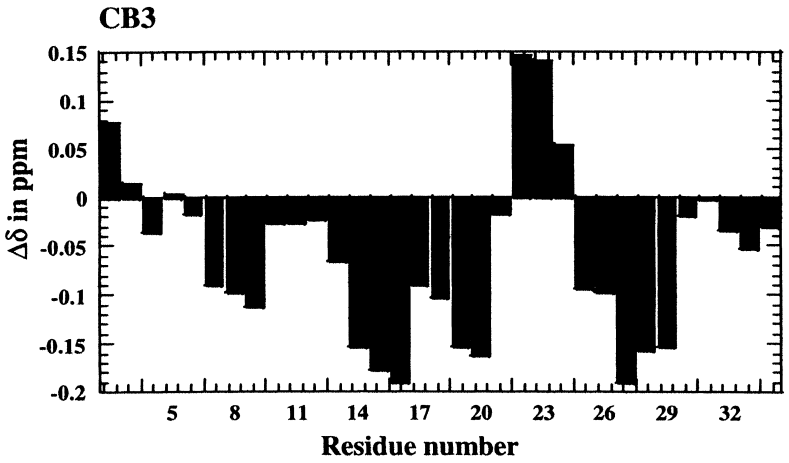

Fig. 4. Up-field chemical shifts of $C_\alpha H$ of CB3 with respect to the values of random-coil shifts [35]. The diagrams were treated by the averages over three neighboring residues excluding the last two residues.

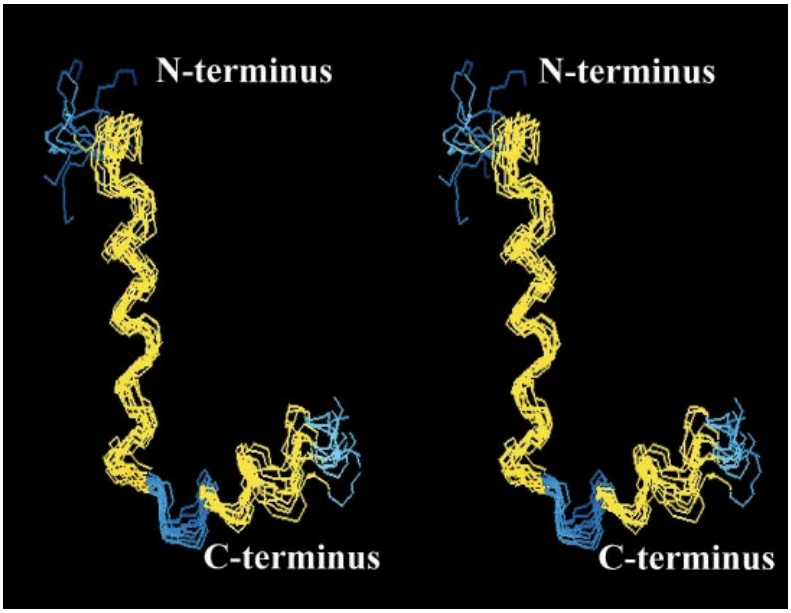

Fig. 5. Stereo view of CB3 showing the backbone superimposition of 12 final simulated annealing structures.

observed in the structure of CB3 owing to the presence of a proline residue at position 25. In addition, the N- and C-terminal ends of the CB3 structure of are frayed with no fixed structure.

DISCUSSION

CB3 was designed to have two hydrophobic α helices, which is different from CB1 having two amphipathic α helices. The NMR structure of CB1 in 20% HFP has been reported previously [24]. Although the three-dimensional structures of both CB1 and CB3 have not per se been determined in a lipid bilayer environment, they nevertheless are expected to provide useful information to rationalize the different actions of these peptides on lipid bilayers. CB3 and CB1 exhibit drastically different actions on anionic lipid vesicles. In an earlier report we demonstrated that CB3 possesses higher lytic activity on liposomes with high content of anionic lipids than CB1 [23]. Similarly, our present results clearly indicate that CB1 has a lower ability to lyse anionic monolayer AOT/isoctane reversed micelles than CB3. These results also imply that CB3 has a more significant interaction with the outward hydrophobic tails of AOT in reversed micelles than CB1. This hydrophobic interaction can be compared to the interaction of hydrophobic tails of lipids.

Comparison of the far UV-CD spectra of CB1 and CB3 show that both the peptides adopt a helical conformation in 20% (v/v) HFP (Fig. 2). The helical content of CB3 appears to be relatively diminished compared to that of CB1. However, the extent of differences in the helical content appear to be unable to explain the observed disparity in the lytic action of these peptides.

The slow but efficient action of CB3 on anionic lipid vesicles could be rationalized based on its structure. As the peptide is mostly hydrophobic, it does not appear to interact with the polar head groups of the anionic lipid vesicles through charge–charge interactions. This aspect probably accounts for the lag in the lytic action of CB3. Interaction of CB3 with inward-facing nonpolar tails is only possible by the inversion of lipids, which consequently leads to cell lysis. Pore formation by CB3 is inhibited due to the discontinuous helix conformation in the peptide. The rather discrete helical segments do not provide an appropriate

environment for strong interactions with the head and tail groups in the lipid bilayer. In addition, the discontinuous helical segments in the structure of CB3 do not favor helix–helix interactions, which is crucial for pore formation. Under these circumstances, CB3 appears to adopt preferentially a different mechanism (i.e. not pore formation) to lyse the anionic lipid bilayers. The drastic perturbation produced in the lipid membrane due to the inversion of the lipids also appears to account for the higher anionic vesicle lytic rate of CB3 as compared to CB1.

The cytotoxicity assays (Table 1) indicate that CB3 has negligible ability to kill both cancer cells and bacteria (IC_{50} values are >50 μM and LC is not available, respectively). Whereas CB1 can effectively lyse these cells (IC_{50} values are between 2.4 and 10.2 μM for cancer cells and LC is <1.48 μM for Gram negative bacteria). Both peptides have difficulty destroying normal cells such as fibroblast cells (IC_{50} values are larger than 50 μM) and erythrocytes (HE_{50} values are larger than 100 μM) and show their therapeutic value. The reasons for the different potencies of these peptides towards cancer cells and bacteria could be due to their structures or sequence and indicate that CB1, with the continuous helical conformation, is likely to interact with cell-surface structures such as microvilli in cancer cells or lipopolysaccharides in bacteria (e.g. strong binding of CB1 with the cell surface is required prior to the lysis of peptide on cell membranes) [22]. However, when purely artificial membranes were used, CB3 with the crumpled helical conformation was found to have higher ability than CB1 to break down the liposomes with higher content of anionic lipids, but not to bind to them [23]. The low potency of CB3 on bacteria and cancer cells may therefore be associated with this nonbinding characteristic. Further experiments will be conducted for the construction of CB3 analogs with discontinuous conformation , increasing the affinity toward the cell surface.

CONCLUSIONS

Membrane lysis induced by custom lytic peptide CB1 having two amphipathic α helical segments and CB3 having two hydrophobic α helical segments on lipid layers has been shown to occur through different pathways [12,23]. The characteristics of residues in the peptides, including net charges and polarity, were found to influence the lytic ability of the peptides on membranes. In this study, NMR structure of CB3 in HFP demonstrates that the helix conformation in the peptide is discontinuous. This discrete α helical conformation of CB3 may provide a structural basis for the different modes of lytic action. Site-specific mutants of CB3 will be designed in the future to enhance the lytic potency of CB3 on cancer cells that have a high content of anionic lipids.

ACKNOWLEDGEMENTS

This work was supported in part by the research fund from Institute of BioAgricultural Sciences at Academia Sinica, Taiwan (H. M. C.) and in part by grants NSC 88-2113-M007-028/NSC 88-2311-B007-021 from National Science Council of Taiwan (C. Y.).

REFERENCES

1. Saberwal, G. & Nagaraj, R. (1994) Cell-lytic and antibacterial peptides that act by perturbing the barrier function of membranes: facets of their conformational features, structure-function correlations and membrane-perturbing abilities. *Biochim. Biophys. Acta* **1197**, 109–131.
2. Maloy, W.L. & Kari, U.P. (1995) Structure–activity studies on magainins and other host defense peptides. *Biopolymers* **37**, 105–122.
3. Hancock, R.E.W. & Lehrer, R. (1998) Cationic peptides: a new source of antibiotics. *Trends Biotech.* **16**, 82–88.
4. Boman, H.G. & Hultmark, D. (1981) Cell-free immunity in insects. *Trends Biochem. Sci.* **6**, 306–309.
5. Hultmark, D., Steiner, H., Rasmuson, T. & Boman, H.G. (1980) Insect immunity: purification and properties of three inducible bactericidal proteins from hemolymph of immunized pupae of *Hyalophora cecropia*. *Eur. J. Biochem.* **106**, 7–16.
6. Boman, H.G. & Hultmark, D. (1987) Cell-free immunity in insects. *Ann. Rev. Microbiol.* **41**, 103–126.
7. Faye, I., Pye, A., Rasmuson, T., Boman, H.G. & Boman, I.A. (1975) Insect immunity. II. Simultaneous induction of antibacterial activity and selection synthesis of some hemolymph proteins in diapausing pupae of *Hyalophora cecropia* and *Samia cynthia*. *Infect. Immun.* **12**, 1428–1438.
8. Chen, H.M., Wang, W., Smith, D.K. & Chan, S.C. (1997) Effects of the anti-bacterial peptide cecropin B and its analogs, cecropins B-1 and B-2, on liposomes, bacteria, and cancer cells. *Biochim. Biophys. Acta* **1336**, 171–179.
9. Steiner, H. (1982) Secondary structure of the cecropins: antibacterial peptides from the moth *Hyalophora cecropia*. *FEBS Lett.* **137**, 283–287.
10. Steiner, H., Andreu, D. & Merrifield, R.B. (1988) Binding and action of cecropin and cecropin analogues: antibacterial peptides from insects. *Biochim. Biophys. Acta* **939**, 260–266.
11. Andreu, D., Merrifield, R.B., Steiner, H. & Boman, H.G. (1985) N-terminal analogues of cecropin A: synthesis, antibacterial activity, and conformational properties. *Biochemistry* **24**, 1683–1688.
12. Hung, S.C., Wang, W., Chan, S.I. & Chen, H.M. (1999) Membrane lysis by the antibacterial peptides cecropins B1 and B3: a spin-label electron spin resonance study on phospholipid bilayers. *Biophys. J.* **77**, 3120–3133.
13. Holak, T.A., Engstrom, A., Kraulis, P.J., Lindeberg, G., Bennich, H., Jones, T.A., Gronenborn, A.M. & Clore, G.M. (1988) The solution conformation of the antibacterial peptide cecropin A: a nuclear magnetic resonance and dynamical simulated annealing study. *Biochemistry* **27**, 7620–7629.
14. Sipos, D., Andersson, M. & Ehrenberg, A. (1992) The structure of the mammalian antibacterial peptide cecropin P1 in solution, determined by proton-NMR. *Eur. J. Biochem.* **209**, 163–169.
15. Shai, Y. (1995) Molecular recognition between membrane-spanning polypeptides. *Trends Biochem. Sci.* **20**, 460–464.
16. Merrifield, R.B., Merrifield, E.L., Juvvadi, P., Andreu, D. & Boman, H.G. (1994) Antimicrobial Peptides. In *Ciba Foundation Symposium* (Marsh, J. & Goode, J.A., eds), pp. 5–20. Wiley, Chichester, UK.
17. Houston, Jr, Kondejewski, M.E., Karunaratine, L.H., Gough, D.N., Fidai, H., Hodges, R.S. & Hancock, R.E.W. (1998) Influence of preformed alpha-helix and alpha-helix induction on the activity of cationic antimicrobial peptides. *J. Pept. Res.* **52**, 81–88.
18. Gazit, E., Lee, W.J., Brey, P.T. & Shai, Y. (1994) Mode of action of the antibacterial cecropin B2: a spectrofluorometric study. *Biochemistry* **33**, 10681–10692.
19. Christensen, B., Fink, J., Merrifield, R.B. & Mauzerall, D. (1988) Channel-forming properties of cecropins and related model

compounds incorporated into planar lipid membranes. *Proc. Natl Acad. Sci. USA* **85**, 5072–5076.

20. Durrel, S.R., Raghunathan, G. & Guy, H.R. (1992) Modeling the ion channel structure of cecropin. *Biophys. J.* **63**, 1623–1631.
21. Mchaourab, H.S., Hyde, J.S. & Feix, J.B. (1993) Aggregation state of spin-labeled cecropin AD in solution. *Biochemistry* **32**, 11895–11902.
22. Chan, S.C., Yau, W.L., Wang, W., Smith, D.K., Sheu, F.-S. & Chen, H.M. (1998) Microscopic observations of the different morphological changes caused by anti-bacterial peptides on *Klebsiella pneumoniae* and HL-60 leukemia cells. *J. Peptide Sci.* **4**, 413–425.
23. Wang, W., Smith, D.K., Moulding, K. & Chen, H.M. (1998) The dependence of membrane permeability by the antibacterial peptide cecropin B and its analogs, CB-1 and CB-3, on liposomes of different composition. *J. Biol. Chem.* **273**, 27438–27448.
24. Srisailam, S., Arunkumar, A.I., Wang, W., Yu, C. & Chen, H.M. (2000) Conformational study of a custom antibacterial peptide cecropin B1: implications of the lytic activity. *Biochim. Biophys. Acta* **1479**, 275–285.
25. Chen, H.M. & Schelly, Z.A. (1995) Laser-induced transient electric birefringence and light scattering in aerosol-OT/CCl_4 reverse micelles. *Langmuir* **11**, 758–763.
26. Bax, A. & Davis, D.G. (1985) MLEV-17-Based two dimensional homonuclear magnetization transfer spectroscopy. *J. Magn. Reson.* **65**, 355–366.
27. Griesinger, C., Otting, G., Wuthrich, K. & Ernst, R.R. (1988) Clean TOCSY for ^{1}H spin system identification in macromolecules. *J. Am. Chem. Soc.* **110**, 7870.
28. Marion, D. & Wuthrich, K. (1983) Application of phase sensitive two-dimensional correlated spectroscopy (COSY) for measurements of ^{1}H-^{1}H spin-spin coupling constants in proteins. *Biochem. Biophys. Res. Comm.* **113**, 967–974.
29. Brunger, A.T., Kuryan, J. & Karplus, M. (1987) Crystallographic R factor refinement by molecular dynamics. *Science* **235**, 458–460.
30. Brunger, A.T., Clore, G.M., Gronenborn, A.M. & Karplus, M. (1987) Solution conformations of human growth hormone releasing factor: comparison of the restrained molecular dynamics and distance geometry methods for a system without long-range distance data. *Protein Eng.* **1**, 399–406.
31. Wüthrich, K. (1986) In *NMR of Proteins and Nucleic Acids*, pp. 130–161. John Wiley and Sons, New York.
32. Brooks, B.R., Brucoleri, R.E., Olafson, B.D., States, D.J., Swaminathan, S. & Karplus, M. (1983) CHARMM: a program for macromolecular energy, minimization and molecular dynamics calculations. *J. Comput. Chem.* **4**, 187–217.
33. Nilges, M., Clore, G.M. & Gronenborn, A.M. (1988) Determination of three-dimensional structures of proteins from interproton distance data by hybrid distance geometry-dynamical simulated annealing calculations. *FEBS Lett.* **229**, 317–324.
34. Nilges, M., Gronenborn, A.M., Brunger, A.T. & Clore, G.M. (1988) Determination of three-dimensional structures of proteins by simulated annealing with interproton distance restraints. Application to crambin, potato carboxypeptidase inhibitor and barley serine proteinase inhibitor 2. *Protein Eng.* **2**, 27–38.
35. Wishart, D.S., Sykes, B.D. & Richards, F.M. (1991) Relationship between nuclear magnetic resonance chemical shift and protein secondary structure. *J. Mol. Biol.* **222**, 311–333.

SUPPLEMENTARY MATERIAL

The following supplementary material is available from http://www.blackwell-science.com/ejb/

Table S1. ^{1}H chemical shifts (p.p.m.) of CB3 in 20% HFP solution.